Accepted for publication at ICOLD European Symposium, Geiranger, Norway, 25-27 June 2001

A new approach for better assessment of rock scouring due to high velocity jets at dam spillways

E. Bollaert & A. Schleiss
Laboratory of Hydraulic Constructions, Swiss Federal Institute of Technology, EPFL, Lausanne, Switzerland

ABSTRACT: High velocity plunging jets, emerging from spillways of large dams, often create erosion of the downstream rock bed. Traditionally, scour is estimated with (semi-) empirical formulae that neglect part of the physics involved. Above all, the relationship between hydrodynamic pressures in rock joints and pressures at the plunge pool bottom is unknown. Experimental tests in simulated closed-end joints, at prototype jet velocities, outlined that scouring is highly dynamic, governed by the interaction of three phases (air-water-rock) and characterized by transient pressure phenomena, such as oscillations and resonance. Based on tensile stress and dynamic uplift, a rock mass failure criterion is proposed for the assessment of scouring. The application of measured dynamic pressures to tensile stress failure criteria, such as the linear elastic (LE) or the fracture mechanics (LEFM) approach, is discussed more in detail. This physically based approach provides a better understanding of the formation of ultimate scour depth.

1 INTRODUCTION

Results of a theoretical and experimental analysis of a research study concerning the pressure fluctuations inside closed-end rock joints, due to the impact of high velocity jets emerging from dam spillways, are presented. A better understanding of these dynamic pressures is necessary to assess the basic physical processes of rock mass destruction by hydrodynamic fracturing and jacking of the existing joints and hydrodynamic uplift of the formed blocks.

Pressure measurements inside artificially created 1D and 2D rock joints were performed which highlighted the formation of violent transient two-phase flow phenomena in the form of standing waves, shock waves and resonance conditions (Bollaert 2001). In that way, extreme pressures inside the rock joints can attain values of up to several times the kinetic energy of the impacting jet. The presence of air bubbles in the pressurized flow on this wave propagation process appears to be of crucial significance, because it highly influences the governing wave celerity and thus makes the problem non-linear (Bollaert & Schleiss 2001).

The actual state-of-the-art on ultimate scour depth evaluation methods comprises empirical and semi-empirical formulas, methods of rock block uplift by applying a maximum possible underpressure combined with a minimum overpressure, and finally the application of realistic instantaneous pressure differentials over and under rock blocks or concrete slabs of protection linings. The existing approaches can be classified with the help of the three phases involved: the liquid phase (water), the gas phase (air) as well as the solid phase (rock). The three-dimensional cube in Figure 1 summarizes the most important existing methods of ultimate scour evaluation and compares them with the objective of the present research and possible future developments. As it can be seen, the challenge is the development of an improved scour evaluation method that accounts for the mentioned physical processes in a 3-phase transient manner.

In the following, special attention will be drawn on the global methodology that is proposed for a more appropriate prediction of ultimate scouring. Above all, the hydrodynamic action of the air-water mixture inside the rock joints has to be defined and applied to appropriate rock failure criteria for the physical-mechanical processes of hydrodynamic fracturing and uplift. The fracturing and jacking process is related to the tensile stress resistance and initial stresses of the rock mass and can be described by a linear elastic stress field or by a fracture mechanics approach (Haimson & Zhao 1991). Uplift is defined as a dynamic equilibrium of forces on a rock block as a function of time, thus procuring the impulsive action that ejects the block.

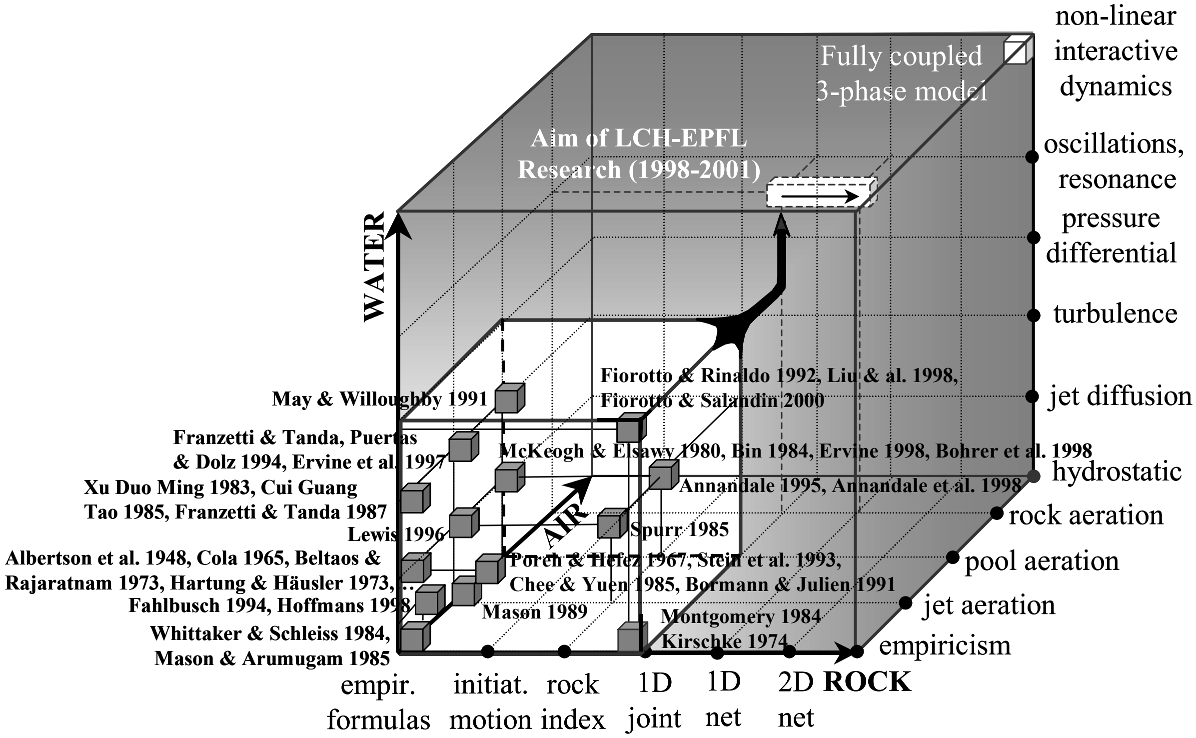

Figure 1. 3D visualization of the actual state-of-the-art on ultimate scour depth evaluation methods and of the LCH-EPFL project's objective (Bollaert & Schleiss 2001).

2 EXPERIMENTAL FACILITY

2.1 General description

The experimental set-up can be divided in two main elements: an upper 3m-diameter cylindrical element in PVC reinforced by a steel structure, and a lower element simulating the joint by a 1 mm thin inox strip that is prestressed with the help of 10 steel bars between two 100 mm thick, 1 ton heavy, galvanized steel plates (Figure 2 and Photos 5b, c).

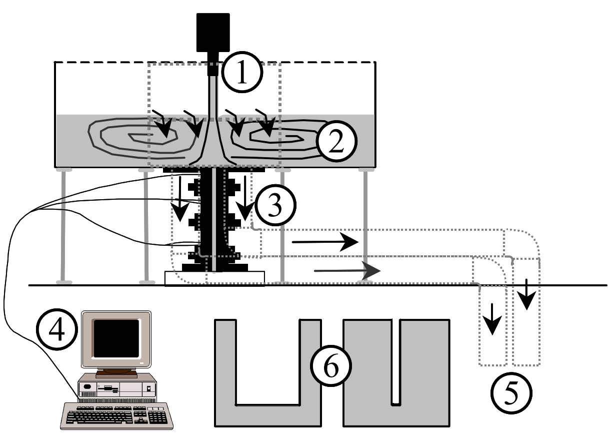

Figure 2. Side view of experimental facility: 1) cylindrical jet outlet, 2) cylindrical basin, 3) pre-stressed two-plate steel structure, 4) PC-DAQ and pressure sensors, 5) restitution system, 6) thin steel strips (1D and 2D fissures).

The jet outlet has diameters of either 57 or 72 mm and is of cylindrical or convergent shape. The water in the basin is restituted over two rectangular sharp weirs that are located radially symmetrically at the border of the basin. 10 pressure sensor taps are installed at the plunge pool bottom and 6 inside the artificial rock joint.

2.2 Jet outlet structure

Two different types of jet outlet configurations were used during the tests (Figure 3). The jet of cylindrical shape has diameters of 57 or 72 mm and a total length of 450 mm. One third of this length is situated inside the upstream water supply conduit, the other two thirds are visible from the outside.

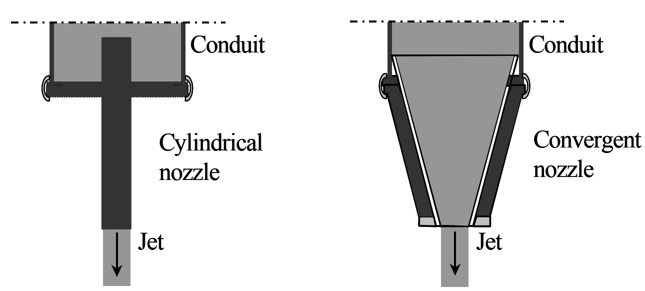

Figure 3. Cylindrical (57 or 72 mm) and convergent (only 72 mm) jet outlet configurations used for the tests.

The second configuration consists of a convergently shaped nozzle of 400 mm long (300 mm outside the water supply conduit) and a diameter that gradually changes from 300 mm to 72 mm.

2.3 Cylindrical basin and lower steel structure

The plastic basin reinforced with steel girders represents the plunge pool and has a water depth that can vary between 0 and 0.7 m, for a total height of 1m (Figure 4).

The lower galvanized steel structure prestresses a 1mm inox strip between two thick plates as shown in Figure 4. This is obtained by the use of a series of 10 prestressable steel bars of 36 mm of diameter (Photo 1a). The inner boundary of the inox strip defines the geometry of the simulated rock joint, while the force induced into the bars automatically provides a watertight sealing.

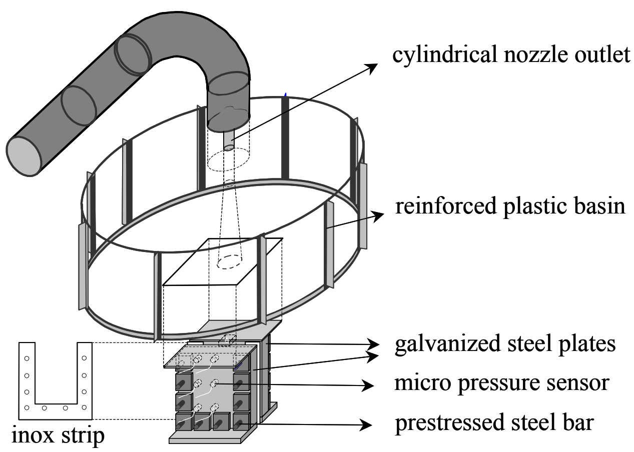

Figure 4. Perspective view of experimental facility presenting the alimentation conduit, the upper plastic basin and the lower steel structure.

The artificially created rock joints are thus one-or two-dimensional, of any particular form, but with a constant thickness. In this paper, only the results for the first type of rock joints, i.e. non-persistent or closed-end rock joints, are presented. This configuration is particulary interesting in view of hydrodynamic fracturing. The second type of joints, i.e. the open-end joints, is of interest when evaluating hydrodynamic uplift of rock blocks. Tests on these joints are actually ongoing. A 1D joint (0.80 m long, 0.01 m wide, 0.001 m thick) and an analogous 2D joint (0.80 m long, 0.60 m wide, 0.001 m thick) were tested. Although they constitute a very simplified representation of realistic rock joints, neglecting parameters as joint apertures and macro-roughness, points of contact, joint walls, filler material, a.s.o. they give a good idea of the pressure characteristics inside. The influence of wall friction along the simulated rock joint, as well as the effect of the modulus of elasticity of the steel ($E_{st} = 2.1 \times 10^{11}$ Pa) on pressure wave celerity or structural vibration, can be neglected in the present analysis.

2.4 Electronic data acquisition equipment

The data acquisition equipment comprises an automatic data measurement system that was specially designed for simultaneous and dynamic signal acquisition and analysis.

The signal conditioning hardware has been developed at the Hydraulic Machines Laboratory (LMH) at the Swiss Federal Institute of Technology (EPFL, Lausanne, Switzerland) and uses an 8-channel platform with the following performances (per channel): programmable sensor excitation and amplification, electrical isolation, jumper-selectable lowpass filtering with different settings, simultaneous 14 bit A-D conversion, and finally routing towards the PC by use of a high speed ARCNET-interface. Each channel can stock up to 65,536 values at maximum 20 kHz acquisition rate.

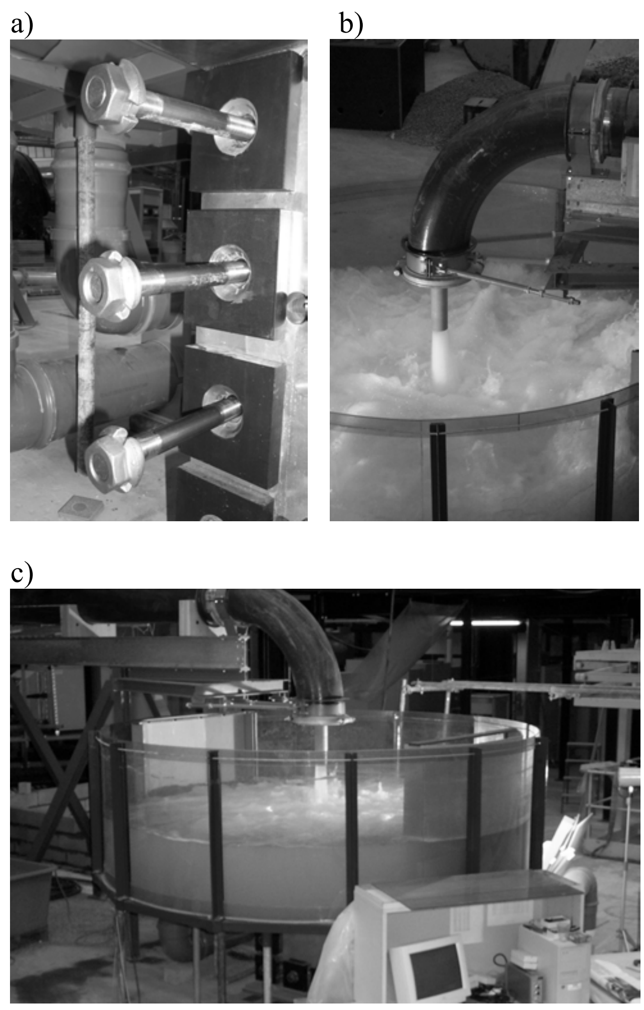

Photo 5. a) View of prestressable steel bars at opened steel structure; b) View of the cylindrical jet operating at an outlet velocity of 15 m/s; c) general view of the experimental facility with PC and DAQ system in the foreground.

The typical acquisition rate is 1 kHz, with a low-pass filtering at 500 Hz, according to the Nyquist theorem. This generates 65 seconds of values for every run and reproduces representative and ergodic statistical values. Regular control runs were performed at acquisition rates of up to 20 kHz in order to check the transient character of the measured pressure peaks.

The used software is written in the LabVIEW environment and has been developed at the Laboratory of Hydraulic Constructions of the EPFL.

The surface mounted micro pressure sensors (3 mm in diameter) are of the piezoelectric type (KULITE XTC-190C), with an absolute pressure range between 0 and 17 bar and a total precision of +/- 0.1% of the full scale output. They can easily be screwed into the steel structure.

With 6 sensor dowels inside the artificially created rock joints and 10 sensor dowels at the plunge pool bottom, an easily changeable system of pressure measurement locations can be obtained.

At the same time, the pressure sensors can be used for pressure measurements directly at the jet outlet to determine initial jet turbulence intensity values.

3 HYDRODYNAMIC CHARACTERISTICS

The first step of a physically based approach of ultimate scour depth evaluation consists of the hydrodynamic action of plunging jet impacts inside pre-existing or created rock joints. Three physical phases are involved and have to be studied: plunging jet characteristics, resulting plunge pool bottom pressure fluctuations and finally the directly depending rock joint pressure fluctuations.

3.1 Characteristics of plunging jet

Table 1 summarizes the most relevant plunging jet characteristics for the 0.072 m diameter cylindrical nozzle outlet used for the experiments. Similar tests were conducted on convergent nozzle outlets but are not presented here because they generated pressure results of the same kind as the cylindrical nozzle.

Attention has to be paid to the small jet fall heights L (max. 0.50 m), and the small degree of break-up L/L_b (max. 0.13) of the jets. Therefore, the generated jets are of a rather compact nature. Furthermore, measured initial turbulence intensities are of around 4 to 5 %. High Reynolds and Weber numbers were obtained, avoiding the influence of viscous and surface tension effects on the results.

Because secondary currents in the upstream conduit system could not be totally avoided, the outcoming jets showed some low frequency (< 1 Hz) instabilities, particularly visible at jet outlet velocities of less than 15 m/s.

Table 1. Plunging jet characteristics for the 72 mm diameter cylindrical nozzle outlet system

V_j	Q_j	Fr	Re	We	T_u	L	L/L_b	L/D_j	Y/D_j
m/s	m^3/s	-	-	%	%	cm	-	-	-
7.4	30	8.8	$4E10^5$	232	4.45	3-50	0.13	0.4-7	2.1-9.7
9.8	40	11.7	$5E10^5$	308	5.45	3-50	0.12	0.4-7	2.1-9.7
12.3	50	14.6	$7E10^5$	386	4.89	3-50	0.11	0.4-7	2.1-9.7
14.7	60	17.5	$8E10^5$	462	4.31	3-50	0.10	0.4-7	2.1-9.7
17.2	70	20.5	$9E10^5$	540	4.25	3-50	0.09	0.4-7	2.1-9.7
19.7	80	23.4	$1E10^6$	619	4.49	3-50	0.09	0.4-7	2.1-9.7
22.1	90	26.3	$1E10^6$	694	4.35	3-50	0.09	0.4-7	2.1-9.7
24.6	100	29.3	$1E10^6$	773	4.37	3-50	0.08	0.4-7	2.1-9.7
27	110	32.1	$2E10^6$	848	4.26	3-50	0.08	0.4-7	2.1-9.7
29.5	120	35.1	$2E10^6$	926	4.39	3-50	0.08	0.4-7	2.1-9.7

3.2 Plunge pool bottom pressure influence on rock joint pressures

The impact of a high velocity jet into a plunge pool is governed by the concept of jet diffusion through a medium at rest. Momentum exchange with the pool generates a progressively growing shear layer, expressed by an increase of the jet's total cross section and a convergence of the jet core region with constant velocity profile (Rajaratnam 1976). Therefore dynamic pressures on the rock-water interface can be generated by direct jet core impact, appearing for small plunge pool depths, or indirectly by the macroturbulent shear layer flow, appearing for ratios of pool depth to jet thickness (Y/D_j) higher than 4 to 6 in the case of plunging jets (Ervine et al. 1998). Terminology used in this paper thus distinguishes between jet core impact and developed jet impact (Figure 6).

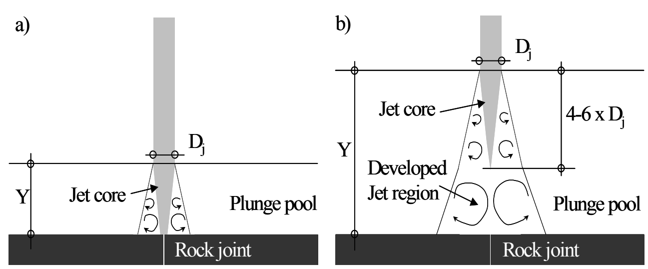

Figure 6. a) jet core impact appearing for $Y/D_j < 4\text{-}6$; b) developed jet impact appearing for $Y/D_j > 4\text{-}6$

The influence of plunge pool bottom pressures on rock joint pressures is governed by a flow modification from macroturbulent conditions into pressurized flow through a bounded medium. The impact of a jet on a joint contains principally all the elements of a resonator system. The problem lies in the excitation capability of the jet. Transient pressures acting on a joint with a length of maximum 10 m and wave celerities of about 1000 m/s can create oscillatory conditions for a frequency range that is slightly beyond 35-70 Hz (fundamental resonance mode $f_r = c_j/(4L_f)$ or $= c_j/(2L_f)$ for closed or open-end resonator, Wylie & Streeter 1978). Resonance is not possible for the macro-turbulent flow in a plunge pool, which has its highest energy at low frequencies (< 25 Hz, Toso & Bowers 1988). The tests performed by the authors indicate however that a high velocity jet has sufficient energy beyond this range to create a resonant excitation inside open or closed-end rock joints (Bollaert 2001). The high air content in plunge pools (Bin 1984, Ervine 1998) and the transfer of flow at the rock-pool interface from macro-turbulent flow into pressurized flow are responsible for considerable air bubble presence inside the rock joints.

This can be explained by alternating air bubble release and re-solution effects of the flow mixture propagating in the joint. In fact, if a liquid with a certain gas content in solution undergoes a pressure drop, supersaturation and thus gas release occurs (Bhallamudi & Chaudry 1990). The amount of released gas directly depends on the pressure drop below the governing saturation pressure and on the degree of agitation of the mixture. A very slight change in free gas drastically changes the mixed fluid compressibility and thus wave celerity.

The air contents inside 1D and 2D simulated rock joints have been quantified by means of the corresponding wave celerity. For jet core impact, the mean free air content stays more or less constant between 0.5 and 2%. This indicates low plunge pool air contents and ineffective pressure drops inside. Developed jet impact allows considerable air bubble release and thus very low wave celerities, even for high mean pressures. Celerities less than 100 m/s and air contents higher than 10 % have been observed.

In Figure 7 a comparison is made between the measured pressure at the plunge pool bottom, next to the rock joint entrance, and the pressure inside a closed-end 1D rock joint. It can be seen that the surface pressure signal gets strongly modulated inside the rock joint. The pressure inside the joint is characterized by the appearance of important oscillatory conditions, giving rise to considerable peak values. These peaks indicate the capability of high velocity jets to create oscillatory and resonance conditions inside underlying rock joints. Their importance highly depends on the macroturbulent flow pattern at the plunge pool bottom and on the available air content that can be released inside the joint. Jet core impact is characterized by low air contents (because not influenced by the surrounding highly aerated shear layer) and relatively moderate pressure changes. Therefore, the obtained peak values are less than those for developed jet impact, which create a combination of highly turbulent flow conditions in the plunge pool, close to the joint entry, with an important available air content. For such conditions, well pronounced resonant phenomena inside the joints, and thus high peak pressures, result.

This is illustrated with Figure 8, in the case of a 1D closed-end joint. The maximum obtained peak pressure values are described by means of a C_{max} coefficient, defined as the ratio of extreme pressure head to the incoming jet's kinetic energy $V^2/2g$. Peak values of up to 5 to 6 times the jet energy injected in the plunge pool were measured inside the joints.

Furthermore, Figure 8 shows a limit of estimated maximum values according to the Y/D_j ratio. At the beginning, the curve grows with increasing Y/D_j, due to increasing pool turbulence and air release, followed by a decrease at $Y/D_j > 10$ due to considerable diffusion of the plunge pool turbulence.

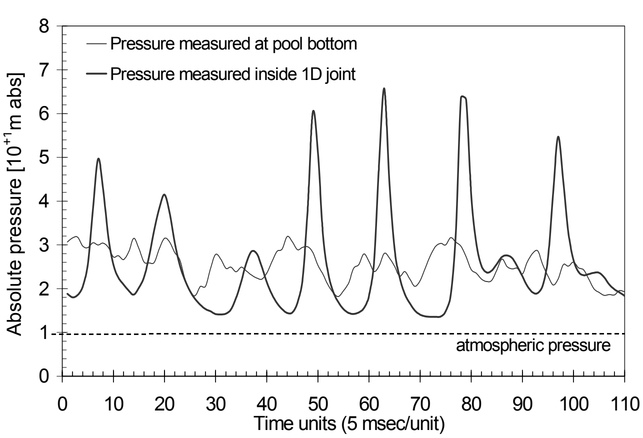

Figure 7. Pressure result in the time domain: comparison of the plunge pool bottom pressure with the corresponding 1D rock joint pressure.

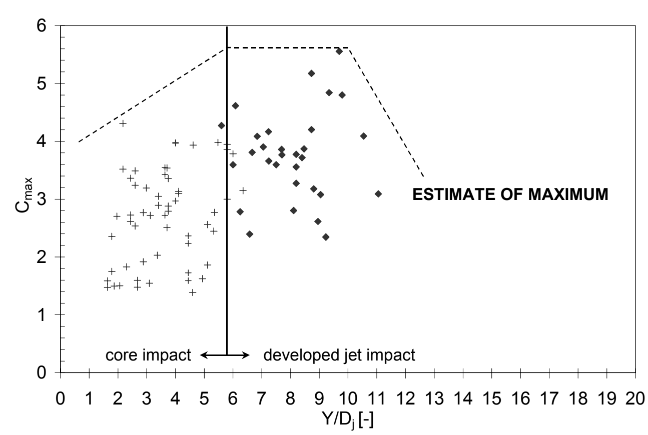

Figure 8. Coefficient C_{max} of extreme peak pressure value in function of the Y/D_j ratio. Curve of estimated extremes for application of failure criteria based on tensile stress (see § 4).

This limiting curve can be used for the estimation of maximum peak pressure values, as required when applying to a failure criterion based on tensile resistance of the rock mass, as explained hereafter in § 4. The input parameters are the impacting jet velocity V_j, the jet diameter D_j and the plunge pool depth Y. All these parameters can be rather easily determined.

4 GEOMECHANICAL CHARACTERISTICS

4.1 *Description of the rock mass*

The analysis of the hydrodynamic action of a high velocity air-water jet on the underlying, jointed rock mass needs an accurate description of the main geomechanical characteristics of the rock itself and of its discontinuities. In the following, only two-dimensional rock mass representations will be considered. Table 2 summarizes the most important parameters necessary to describe how the rock mass will resist against the hydrodynamic forces. Most of the parameters can be obtained by simple field observations and borehole tests. The parameter TYPE is related to the crystallographic composition of the rock mass whereas STRUC refers to the evolution of this composition according to depth (Table 2).

Table 2. Main geomechanical parameters of the rock mass

Parameter	Symbol	Dim
Rock mass type	TYPE	[-]
Rock mass structure	STRUC	[-]
Depth of layer	H_l	[m]
Rock Quality Designate	RQD	[%]
Uniaxial compressive strength	σ_c	[MPa]
Uniaxial tensile strength	σ_t	[MPa]
Young's modulus of elasticity	E_r	[MPa]
Material density	ρ	[kg/m^3]
Number of joint sets	N_j	[-]
Joint set dip angle	α_j	[°]
Joint set persistency	P_j	[%]
Joint set typical length	L_j	[m]
Joint set spacing	S_j	[m]
Joint set width	e_j	[m]
Joint set friction angle	φ_j	[°]

The rock mass structure STRUC allows a subdivision of the rock mass into different layers of a certain type of mineralogy and of a certain depth H_l. For each of the layers, it is essential to know how the internal layer parameters are interrelated.

Figure 9 illustrates in a two-dimensional way the two mostly encountered layer situations: in Figure 9a, a non-persistent rock mass pattern is shown, characterized by two ($N_j = 2$) joint sets that only intersect at some of their joints. In other words, the potential 2D-joint pattern of the rock mass is not fully established and certain joints are of the so-called "closed-end" type. These rocks have joint set persistencies P_j less than 100 %.

The second layer (Figure 9b) represents a much more completed stage of rock mass break-up, i.e. the 2D-joint pattern is completely established and the fully persistent (P_j = 100 %) rock mass can be subdivided into a large number of similarly shaped, regularly distributed rock cubes. Despite the persistent joint pattern, local contact surfaces between the blocks exist.

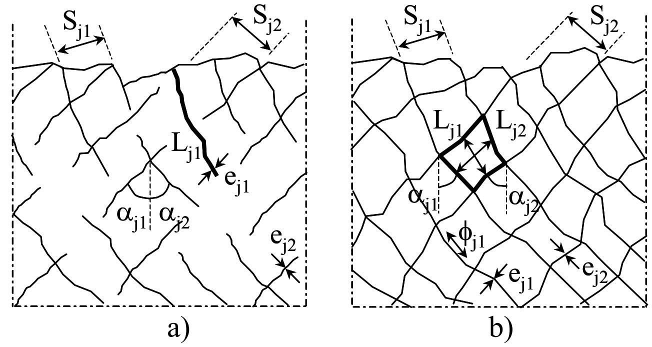

Figure 9. Two often encountered rock mass layer situations: a) non-persistent joint set pattern (P_j < 100 %); b) persistent joint set pattern (P_j = 100 %)

When assuming that physical-mechanical processes are responsible for rock mass destruction and thus for scour hole development, it is obvious that the behavior of the non-persistent rock mass is highly governed by the hydrodynamic fracturing principle. In order to express the resistance of such a rock mass, it is necessary to relate these forces with a failure criterion expressing whether the joint will propagate or not. This aspect has been largely investigated by linear elastic (LE) tensile stress theory, often used to determine in-situ horizontal stresses, and by (static) hydraulic fracturing techniques, mainly used in the petroleum industry, and based on a linear elastic fracture mechanics (LEFM) approach. However, the particularity of the present application lies in the highly dynamic character of the impacting hydrodynamic forces: the rate of application generally modifies the static fracture propagation resistance of a rock mass and should be taken into account in a fully dynamic analysis.

In the case of a completely fissured rock mass, its resistance against hydrodynamic failure can be expressed by some typical rock block characteristics, such as size, shape, weight and shear and/or cohesive forces along the joints. This resistance can thus be introduced in a dynamic equilibrium of the forces acting on the rock block. This equilibrium will highly depend on the instantaneous difference in pressure distribution above and underneath the block and therefore has to be formulated in function of time (impulse). The calculated net impulse of a pressure wave under a block will determine whether the considered typical rock block will be uplifted out of its matrix or not.

For each of the aforementioned failure types, the ultimate scour hole development can be estimated as follows. Firstly, maximum scour will be reached when the pressure peaks in the closed-end joints are not capable to propagate the joint further anymore. Secondly, for the uplift criterion, scour will be finished when the equilibrium of forces in function of time doesn't allow to push a rock block out of the mass anymore. In the following, each of these failure criteria will be discussed more in detail.

4.2 *Non-persistent rock mass failure criteria*

The presented failure criteria arte limited to the assumption of pure tensile modes of loading (mode I), without any shear force effects. The criteria are essentially based on the parameter P_{b0}, named as "breakdown pressure under zero initial pore pressure and zero far-field stresses", also called the "zero breakdown pressure" (Haimson & Zhao 1991).

Concerning joint tensile failure, two major approaches can be distinguished. The first is the linear elastic (LE) theory which considers the rock mass to be linear elastic, homogeneous, isotropic, initially continuous and impermeable to the fluid. It neglects plastic yielding of the rock and is based on a straightforward comparison of the stresses induced close to the joint end (by the hydrodynamic action) with the in-situ stresses σ_h and σ_H (minor and major principal stresses in a plane perpendicular to the joint) and the tensile strength σ_t of the rock mass. This statement determines the so-called "breakdown pressure P_b" and is formulated in the following manner (Hubbert & Willis 1957, cited in Haimson & Zhao 1991):

$$P_b = \sigma_t + 3\sigma_h - \sigma_H - P_0 \tag{1}$$

with P_0 the local initial pore pressure. It has to be underlined that the zero breakdown pressure P_{b0} corresponds to the rock mass tensile strength σ_t and thus represents a constant rock mechanical property.

This method is often used in order to estimate the in-situ horizontal stress field by means of vertical borehole hydraulic fracturing or jacking tests. For an uncracked rock, such tests are useful to determine in a direct way the hydraulic fracturing breakdown pressure P_b, without particular knowledge on the in-situ stress field (near the surface often neglectable).

The second approach of rock joint tensile failure is based on linear elastic fracture mechanics (LEFM). The major difference with LE theory is the assumption that the zero breakdown pressure P_{b0} gets joint size-dependent and thus is not a constant material property anymore. The expression for the breakdown pressure becomes (Rummel 1987, cited in Haimson & Zhao 1991):

$$P_b = K_{Ic} + k_1\sigma_h + k_2\sigma_H - P_0 \tag{2}$$

with K_{Ic} the "fracture toughness" (for plane strain conditions and mode I fracturing) and k_1 and k_2 both parameters depending on the joint geometry. The breakdown pressure P_b can now be replaced by a constant that gives an idea about the magnitude of the elastic stress field induced by the hydrodynamic force distribution along the joint. This constant is the "stress intensity factor" K_I and is linearly related to the hydrodynamic action (stress σ) and directly related to the square root of a characteristic length, often chosen as the joint length L_j. With reference to Figure 9b for the used parameters, this is mathematically expressed as (Ewalds & Wanhill 1986):

$$K_I = \sigma \cdot \sqrt{\pi L_{j1}} \cdot f\left(\frac{L_{j1}}{S_{j2}}\right) \tag{3}$$

with f(x) a function of the actual length of the joint (L_{j1}) and its maximum possible length (S_{j2}). Joint propagation will only occur when the product of stress times the square root of the joint length attains a critical value. LEFM analysis thus allows to take into account the joint geometry based on a classical linear elastic stress analysis. Furthermore, it can characterize to some extent the processes of subcritical joint propagation, such as fatigue.

Regardless of the adopted failure criterion, the best way to obtain realistic results would be to perform classical hydraulic fracturing or jacking borehole tests, in order to determine at which pressure the pre-existing joints will propagate. This could be done at different depths, depending on the rock structure STRUC and the layer depths H_l, and results in static fracture toughness values $K_{Ic,stat}$ for every layer.

However, depending on the rate of application of the hydrodynamic forces, physically correct joint propagation has to take into account dynamic effects, modifiying both the rock's modulus of elasticity E_r and its tensile strength σ_t. A rate of pressure raise R_p [MPa/s] can be taken into account by performing laboratory dynamic fracturing tests on rock specimens (Haimson & Zhao 1991, Zhao & Li 2000).

It may be concluded that the use of rock joint failure criteria in practice is particularly interesting when hydraulic fracturing or jacking tests can be carried out in-situ. They should be performed at different depths, following the layered structure of the rock mass. The most reliable test results could be obtained by performing dynamic fracturing borehole tests, taking into account the influence of the rate of pressure raise on the fracture toughness. But those are difficult to realize. If no tests can be made, the analysis has to be based on available values of similar rock formations regarding the tensile strength of the rock mass, the local initial pore pressure and the in-situ minimum stresses. A first order estimate can nevertheless be obtained by neglecting the in-situ stress, thus by only taking into account the tensile strength and an initial pore pressure.

4.3 *Persistent rock mass failure criteria*

The second type of failure criteria refers to totally broken-up rock masses. The approach is based on the definition of a representative rock block geometry, called the "characteristic block" (Figure 9b). This block will be subject to a dynamic equilibrium of all the forces acting on as a function of time. The most relevant forces are:

1) The stabilizing force G_b, defined as the immerged weight of the rock block.
2) $F_o(x,t)$, which is defined as the force resulting from the time and space dependent pressure distribution acting over the block. This force results from the macroturbulent pressure pattern in the plunge pool and can under certain conditions be destabilizing when reaching negative values.
3) The stabilizing force which is expressed by the shear force $F_{sh}(t,e_j)$. This force depends on several parameters, such as joint roughness, aperture, filler material, etc. It can be approximately assumed only depending on joint width and time.
4) The most important destabilizing force results from the time, space and joint width dependent pressure distribution F_u (x, t, $e_{j1}(t)$, $e_{j2}(t)$), acting along the joints under the block. This distribution is highly influenced by 2-phase transient phenomena such as oscillations, resonance, a.s.o.

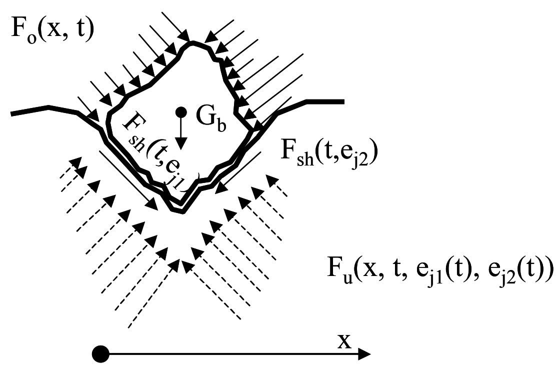

Figure 10. Force balance on a characteristic block

The significant time dependence of all of the above forces requires determination of the dynamic, time dependent impulse on the rock block. The total impulse $I_{\Delta tpulse}$ on the block during the time interval Δt_{pulse} of a certain pressure pulse is obtained by integrating the net force equilibrium at every time step dt, in a defined direction. This defines the final velocity $V_{\Delta tpulse}$ and thus the total uplift height of the block (m = mass of the block):

$$I_{\Delta tpulse} = \int_0^{\Delta tpulse} \left(F_u - F_o - G_b - F_{sh}\right) \cdot dt = m \cdot V_{\Delta tpulse} \qquad (4)$$

In this equation, the pressure distributions above and underneath the block have been spatially integrated in the calculation direction of the force.

Destabilization and thus uplift of the rock block is clearly governed by the pressure differences that can appear during the considered time interval. This pressure difference depends on two aspects that are difficult to determine: first of all the relationship between the overpressure distribution and the plunge pool macroturbulence, and secondly the influence of the change of the joint width during block uplift on the pressure under the block at subsequent time steps. The former depends on the ratio of plunge pool eddy size compared to rock block size and can be obtained by statistical analysis of model tests. This ratio continuously changes during the uplift process, in function of the time evolution of the impulsion. As a first approximation, a conservative result is obtained by neglecting these pressure drops, therefore assuming a pressure under the block that is independent of the block movement, and by applying a maximum negative pressure at the upperside of the rock block. This will result in an upper limit of ultimate scour hole depths.

A more realistic equilibrium of forces will be worked out by the authors, based on ongoing model tests with open-end rock joints. This will allow evaluation of the maximum possible impulsion on a block in function of jet, pool and joint parameters.

5 POSSIBLE APPROACH FOR A NEW ULTIMATE SCOUR METHODOLOGY

Based on the hydrodynamic action inside rock joints (chapter 3) and on rock mass failure criteria (chapter 4), a possible new approach for better assessment of ultimate scour hole development is outlined. At the time of writing, measurements of impulsion on rock blocks were not yet completed. In result, the here proposed methodology is restricted to non-persistent rock masses.

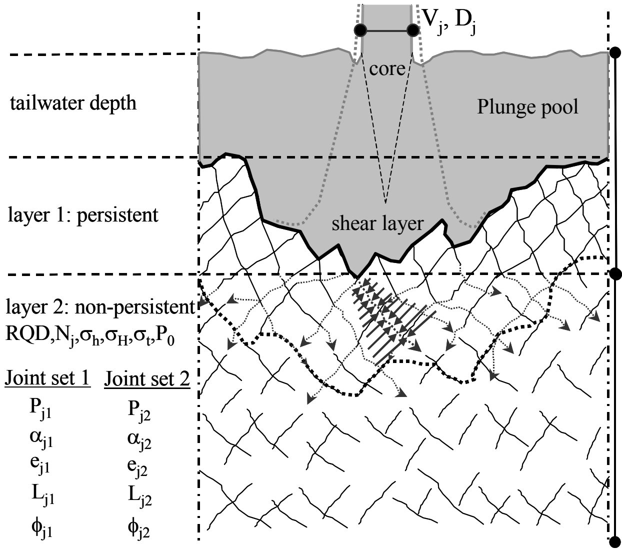

Figure 11. Example of 2-layered rock mass showing the initial plunge pool-rock mass interface (continuous line) and the calculated ultimate scour elevation (dotted line).

An example of a two-layered rock mass is shown in Figure 11. The first rock layer is of the persistent type and has already been scoured out by the impacting jet. It corresponds to the initial condition for the analysis. The second layer is still non-persistent and is formed by two main joint sets ($N_j = 2$). Each joint set has its own parameters and will be loaded by a hydrodynamic action. This action is determined step-by-step, firstly based on the ratio of plunge pool depth to jet impact diameter Y/D_j. Every step of the analysis considers a sublayer with a height corresponding to the characteristic rock block size that will develop. For a given Y/D_j ratio, the extreme positive pressure coefficient C_{max}, as defined in Figure 8, is obtained. Multiplying this coefficient with the incoming kinetic energy of the jet (depending on the jet impact velocity V_j) automatically results in a (dimensional) extreme pressure and thus maximum stress σ_{max} inside the joint. This extreme pressure value will then be compared with the maximum admissible stress in the joint σ_{adm}, obtained by in-situ fracturing or jacking tests.

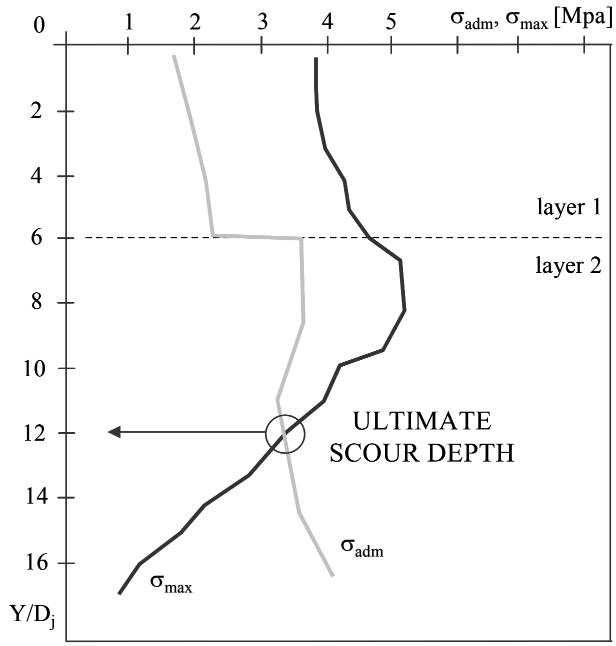

Figure 12. The maximum hydrodynamically induced stress σ_{max} and the admissible rock mass stress σ_{adm} (in function of Y/D_j) graphically determines the ultimate scour hole depth.

This analysis can be repeated several times, sublayer per sublayer, until the maximum hydrodynamic stress in the joint is less than the admissible stress, thus not able to propagate the joint anymore. This comparison is illustrated with Figure 12. The location where the two curves intersect indicates the approximate elevation of the ultimate scour hole bottom as a function of Y/D_j. If the initial stress in the rock is influenced only by overburden pressure, progressing scouring development of course will change the initial stress conditions.

This approach is purely static and doesn't take into account the fatigue effects in the fracture growing zone in front of the fracture tip, nor for dynamic effects induced by the rate of pressure raise R_p.

6 CONCLUSIONS

A possible new approach for better assessment of ultimate scour depth was outlined, based on a detailed analysis of the physical-mechanical processes of hydrodynamic fracturing and jacking, i.e. rock joint propagation, and hydrodynamic uplift of rock blocks. Extreme pressure values inside 1D closed-end rock joints were determined, based on experiments carried out with prototype jet velocities. These values were then introduced in a tensile failure criterion of the rock mass.

For the time being, the proposed general approach of ultimate scour depth evaluation only deals with non-persistent rock masses and is based on a graphical comparison of the maximum hydrodynamical induced stress σ_{max} with the admissible stress σ_{adm} inside the joints, as a function of the ratio of plunge pool depth to jet diameter Y/D_j.

REFERENCES

Bhallamudi, M.S. & Chaudry, M.H. (1990). Analysis of Transients in Homogenous Gas-Liquid Mixtures. *Proceedings of the 6th Int. Conference on Pressure Surges*. BHRA. UK.

Bin, A.K. 1984. Air Entrainment by Plunging Liquid Jets, *Proceedings of the IAHR Symposium on scale effects in modeling hydraulic structures*: paper 5.5-1. Esslingen.

Bollaert, E. 2001. Spectral Density Modulation of Plunge Pool Bottom Pressures inside Rock Fissures. Paper submitted to the *XXIXth IAHR Congress*. Beijing. China.

Bollaert, E. & Schleiss, A. 2001. Air Bubble Effects on Transient Water Pressures in Rock Fissures due to High Velocity Jet Impact. Paper submitted to the *XXIXth IAHR Congress*. Beijing. China.

Ervine, A. 1998. Air Entrainment in Hydraulic Structures: A Review. *Proceedings Institution of Civil Engineers*, *Wat., Marit. & Energy* 130: 142-153.

Ervine, D.A. et al. 1998. Pressure Fluctuations on Plunge Pool Floors. *Journal of Hydraulic Research* 35 (2): 257-279.

Ewalds, H.L. & Wanhill, R.J.H. (1986). Fracture Mechanics. Netherlands: *Delftse Uitgevers Maatschappij*.

Haimson, B.C. & Zhao, Z. (1991). Effect of Borehole Size and Pressurization Rate on Hydraulic Fracturing Breakdown Pressure. *Proceedings of the 32nd US Symposium on Rock Mechanics*. Rotterdam: Balkema.

Rajaratnam, N. 1976. *Turbulent Jets*. Netherlands : Elsevier.

Toso, J.W.; Bowers, C.E. (1988). Extreme Pressures in Hydraulic Jump Stilling Basins. ASCE. *Journal of Hydraulic Engineering*, Vol. 114, N° 8: 829-843.

Wylie, E.B. & Streeter, V.L. 1978. *Fluid Transients*. USA: McGraw-Hill Inc.

Zhao, Z. & Li H.B. (2000). Experimental Determination of Dynamic Tensile Properties of a Granite. *International Journal of Rock Mechanics and Mining Sciences*, Vol. 37: 861-866.